eNeuro

Research Article: New Research | Development

Homeostatic recovery of embryonic spinal activity initiated by compensatory changes in resting membrane potential

https://doi.org/10.1523/ENEURO.0526-19.2020

Cite as: eNeuro 2020; 10.1523/ENEURO.0526-19.2020

Received: 14 December 2019
Revised: 8 May 2020
Accepted: 22 May 2020

Title Page

1.Manuscript Title: Homeostatic recovery of embryonic spinal activity initiated by compensatory changes in resting membrane potential.

2. Abbreviated Title: Homeostatic intrinsic plasticity *in vivo*.

3. List of all Authors Names and Affiliations in order as they would appear in the published article:

Carlos Gonzalez-Islas + #, Miguel Angel Garcia-Bereguiain+ ¶, and Peter Wenner +.

+ Physiology Department. Emory University, School of Medicine, Atlanta, GA, 30322

Doctorado en Ciencias Biológicas. Univerisdad Autónoma de Tlaxcala. Tlax. Mexico

¶ Current address - One Health Research Group. Universidad de Las Americas. Quito. Ecuador.

4. Author Contributions: CG-I and PW **Designed Research**; CG-I, MAG-B and PW **Performed Research**; CG-I, MAG-B and PW **Analyzed Data**; CG-I and PW **Wrote the Paper.**

5. Correspondence should be addressed to:

Peter Wenner (Orcid ID 0000-0002-7072-2194)

Department of Physiology.

Room 601. Whitehead Bldg.

Emory University, School of Medicine,

Atlanta, GA, 30322

Phone (404) 727-1517

Fax (404) 727-2648

Email pwenner@emory.edu

6. Number of figures: 10 and 3 Extended Data Figs

7. Number of Tables: 1

8.Number of Multimedia: 0

9. Number of Words for Abstract: 248

10. No. of words Significant Statement: 120

11. No. of words for Introduction: 689

12. No. of Words for Discussion: 1614

13. Acknowledgements: We thank Drs. Mark Rich and Morten Raastad for their valuable comments on the manuscript.

14. Conflict of Interest: Authors report no conflict of Interest

15. Funding sources: This research was supported by Grants from the National Institute of Neurological Disorders and Stroke (R01NS065992) to P. Wenner.

Abstract (248)

When baseline activity in a neuronal network is modified by external challenges, a set of mechanisms is prompted to homeostatically restore activity levels. These homeostatic mechanisms are thought to be profoundly important in the maturation of the network. It has been shown that blockade of either excitatory GABAergic or glutamatergic transmission in the living chick embryo transiently blocks the movements generated by spontaneous network activity (SNA) in the spinal cord. However, the embryonic movements then begin to recover by 2 hours and are completely restored by 12 hours of persistent receptor blockade. It remains unclear what mechanisms mediate this early recovery (first hours) after neurotransmitter blockade, or even if the same mechanisms are triggered following GABAergic and glutamatergic antagonists. Here we find two distinct mechanisms that could underlie this homeostatic recovery. First, we see a highly robust compensatory mechanism observed shortly after neurotransmitter receptor blockade. In the first two hours of GABAergic or glutamatergic blockade *in vitro* there was a clear depolarization of resting membrane potential in both motoneurons and interneurons. These changes reduced threshold current and were observed in the continued presence of the antagonist. Therefore, it appears that fast changes in resting membrane potential represent a key fast homeostatic mechanism for the maintenance of network activity. Second, we see a less consistent compensatory change in the absolute threshold voltage in the first several hours of *in vitro* and *in vivo* neurotransmitter blockade. These mechanisms likely contribute to the homeostatic recovery of embryonic movements following neurotransmitter blockade.

Significance (120)

Homeostatic plasticity represents a set of mechanisms that act to recover cellular or network activity following a challenge and is thought to be critical for the developmental construction of the nervous system. The chick embryo afforded us the opportunity to observe the timing of homeostatic recovery of network activity following 2 distinct perturbations in a living developing system. Because of this advantage, we have identified a novel homeostatic mechanism that actually occurs as the network recovers and is therefore likely to contribute to nervous system homeostasis. We found that a depolarization of the resting membrane potential and a hyperpolarization of threshold voltage in the first hours of the perturbation enhances excitability and supports the recovery of embryonic spinal network activity.

78

79 **Introduction (689)**

80 Recent work has focused on the mechanisms that allow networks to
81 homeostatically maintain their activity levels in the face of various perturbations (Marder
82 and Goaillard, 2006; Turrigiano, 2011; Davis, 2013). Typically, activity is altered for 24
83 hours or more and compensatory changes in intrinsic cellular excitability and/or synaptic
84 strength (synaptic scaling) are observed following the perturbation. While most of the
85 work has been carried out *in vitro*, homeostatic mechanisms have also been observed
86 *in vivo* in the spinal cord (Gonzalez-Islas and Wenner, 2006; Knogler et al., 2010),
87 hippocampal (Echegoyen et al., 2007), auditory (Kuba et al., 2010) and visual systems
88 (Desai et al., 2002; Goel et al., 2006). The chick embryo spinal cord expresses a
89 spontaneously occurring network activity (SNA) that drives embryonic movements
90 (O'Donovan, 1999; Blankenship and Feller, 2010). SNA likely occurs in all developing
91 circuits shortly after synaptic connections form. In the embryonic spinal cord this activity
92 is a consequence of the highly excitable nature of the nascent synaptic circuit where
93 GABAergic neurotransmission is depolarizing and excitatory during early development
94 (Ben-Ari et al., 1989; O'Donovan et al., 1998; O'Donovan, 1999; Rivera et al., 1999;
95 Blankenship and Feller, 2010). Spinal SNA is known to be important in motoneuron
96 axonal pathfinding (Hanson and Landmesser, 2004), and for proper muscle and joint
97 development (Ruano-Gil et al., 1978; Toutant et al., 1979; Roufa and Martonosi, 1981;
98 Persson, 1983; Hall and Herring, 1990; Jarvis et al., 1996).

99 The embryonic spinal cord provides an exceptional model of homeostasis. Many
100 years ago it was demonstrated that SNA expressed in the isolated spinal cord was

transiently blocked by either glutamatergic or $GABA_A$ receptor (GABAR) antagonists, but within hours was homeostatically restored in the presence of that antagonist (Barry and O'Donovan, 1987; Chub and O'Donovan, 1998). However, the mechanisms of this recovery have not been identified. Interestingly, a similar homeostatic recovery of SNA-generated embryonic movements following neurotransmitter antagonists has also been demonstrated *in vivo* (Wilhelm and Wenner, 2008). When $GABA_A$ or glutamate receptor antagonists were injected into the egg at embryonic day 8 (E8), SNA-driven embryonic movements were abolished for 1-2 hours, but then homeostatically recovered to control levels 12 hours after the onset of pharmacological blockade of either transmitter (Wilhelm and Wenner, 2008). Therefore, it would be expected that mechanisms that contribute to the homeostasis of activity in the living system will have occurred by 2-12 hours of treatment. Because the recovery was very similar following either GABAergic or glutamatergic blockade, one might think that similar mechanisms would drive the recovery of embryonic activity following injection of either antagonist, but this did not appear to be the case. It was determined that following 12 hours of $GABA_A$ receptor blockade compensatory changes in intrinsic excitability were observed (increased Na^+ channel, and a decrease of two different K^+ channel currents – I_A & Ik_{Ca}), although changes in quantal amplitude were not observed until 48 hours of receptor blockade (Wilhelm and Wenner, 2008; Wilhelm et al., 2009). On the other hand following 12 hour glutamatergic blockade no changes in intrinsic excitability were observed, and even after 48 hours of glutamatergic blockade no change in quantal amplitude was seen.

Previous studies had not examined the possibility that compensatory changes in cell excitability and/or scaling were occurring at the onset and throughout the recovery

process in motoneurons. In fact, very few studies have compared the expression of presumptive homeostatic mechanisms with the timing of the homeostatic recovery of activity, yet we would expect that some of these mechanisms would be expressed at the very onset of the recovery process. Further, there is little known about compensations that may be occurring in the interneurons that contribute to the drive of SNA. Therefore, we set out to identify the mechanisms that are expressed during the actual period of homeostatic recovery of SNA. We found some changes in threshold voltage, but importantly we describe a previously unrecognized mechanism of homeostatic intrinsic plasticity where fast changes in resting membrane potential (RMP) bring both interneurons and motoneurons closer to action potential threshold. The results suggest that compensatory changes in RMP could facilitate the homeostatic recovery of activity during glutamatergic or GABAergic blockade in the living embryo.

Methods.

Dissection.

*E*mbryonic day 10 (E10 or stage 36 (Hamburger and Hamilton, 1951)) chick spinal cords were dissected under cooled (15°C) Tyrode's solution containing the following (in mM): 139 NaCl, 12 D-glucose, 17 NaHCO3, 3 KCl, 1 MgCl2, and 3 CaCl2; constantly bubbled with a mixture of 95% O2-5% CO_2 to maintain oxygenation and pH around 7.3. After the dissection, the cord was allowed to recover overnight in Tyrode's solution at

18°C. The next day the cord was transferred to a recording chamber and continuously perfused with Tyrode's solution heated to 27°C to allow for the expression of bouts of SNA with a consistent frequency.

Electrophysiology.

Whole-cell current clamp recordings were made from spinal motoneurons localized in lumbosacral segments 1-3 and were identified by their lateral position in the ventral cord. Recordings were also made from interneurons in the same segments, but these were identified by their more medial position in the ventral cord. Patch Clamp tight seals (1-3 GΩ) were obtained using electrodes pulled from thin-walled borosilicate glass (World Precision Instruments, Inc) in two stages, using a P-87 Flaming/Brown micropipette puller (Sutter Instruments) to obtain resistances between 5 and 10 MΩ. Once whole-cell configuration was achieved, voltage clamp at -70mV was maintained for a period of 5 minutes to allow stabilization before switching to current clamp configuration at which point the RMP was measured. A liquid junction potential of -12 mV was experimentally measured (Neher, 1992) for our conditions. All reported RMP and Threshold values were then corrected offline. In some cases, whole cell voltage clamp recordings were also obtained from motoneurons and interneurons in order to acquire miniature postsynaptic currents (mPSCs) and these recordings were obtained for the first 5-10 minutes of the recording before switching to current clamp to record measures of excitability. Series resistance during the recording varied from 15 to 20 MΩ among different neurons and was not compensated. Voltage clamp recordings were terminated whenever significant increases in series resistance (> 20%) occurred or

when holding current became larger than 50 pA. Cell capacitance was not compensated. Currents were filtered online at 5 kHz and digitized at 10 kHz. AMPA and GABA mPSCs were separated by their decay kinetics as described previously (Gonzalez-Islas and Wenner, 2006). The mPSCs with decay time constants (τ) under 7 ms were counted as AMPAergic and those with τs over 10 ms were counted as GABAergic (Gonzalez-Islas and Wenner, 2006). We did not add TTX to isolate mPSCs in this study because the frequency and amplitude of spontaneous events (no TTX) and mPSCs in the presence of TTX have been shown to be the same (Chub and O'Donovan, 2001; Gonzalez-Islas and Wenner, 2006). The mPSCs were acquired on an Axopatch 200B patch clamp amplifier (Molecular Devices), digitized (Digidata 1200, Molecular Devices) on-line using PClamp 10 (Molecular Devices), and analyzed manually using Minianalysis software (Synaptosoft). For these recordings, if peak to peak noise was larger than 5 pA or the RMS was larger than 1 pA, then the recording was not included in the analysis. The mPSCs were identified automatically by Minianalysis using the following parameters: Threshold: 5pA, Period to search a local maximum: 50 ms; Time before a peak for baseline: 10 ms; Period to search for a decay time: 35 ms; Fraction of peak to find a decay time: 0.37 Period to average a baseline 5ms; Area threshold 10; Number of point to average peak 7; Direction of peak; Negative. We then went through these mini waveforms and accepted them or rejected them following visual inspection of the waveform. Charts and associated average values were obtained by determining an average mPSC amplitude for each cell (variable number of mPSCs/cell, 5pA cutoff), and then calculating the average of all cells. Recordings in current clamp were terminated whenever significant increases in

input resistance (>20%) occurred. Current Clamp recordings were filtered online at 10 kHz, digitized at 20 kHz. The intracellular patch solution for both current and voltage clamp recordings contained the following (in mM): 5 NaCl, 100 K-gluconate, 36 KCl, 10 HEPES, 1.1 EGTA, 1 $MgCl_2$, 0.1 $CaCl_2$, 1 Na_2ATP, and 0.1 MgGTP; pipette solution osmolarity was between 280 and 300 mOsm, and pH was adjusted to 7.3 with KOH. Standard extracellular recording solution was Tyrode's solution (see above), constantly bubbled with a mixture of 95% O2-5% CO_2. In order to obtain rheobase, threshold voltage, and F-I relationships in embryos treated with saline or gabazine *in ovo*, a step protocol was employed (1sec duration, 1pA increments for threshold/rheobase or 5pA increments for the FI curve, at 0.1Hz). To expedite this process so we could get more accurately timed measures of rheobase and threshold voltage following *in vitro* application of gabazine, a ramp protocol (from 0 to 200 pA; 1.2 sec duration at 0.2 Hz; n=3) was used. A test pulse was delivered 800 ms before every step pulse or ramp, a 200ms hyperpolarizing current step of 20 pA was applied, and this provided our measure of input resistance, and also served as an indicator of the reliability of the step. The RMP values were taken as an average of the Vm read at the beginning each sweep in these protocols. Although most of the experiments were not blinded, in 4 experiments the drug application *in ovo* was done blindly to corroborate the results.

In ovo and vitro drug injections.

A window in the shell of the egg was opened to allow monitoring of chick embryo movements and drug application 6 or 12 hrs before isolating the spinal cord at E10. 50 µl of a 10mM gabazine solution was applied onto the chorioallantoic membrane of the

chick embryo to a final concentration of ~10μM, assuming a 50 ml egg volume. For the *in vitro* drug application, 10μM gabazine or 20μM CNQX and 50μM APV was added to the perfusate after recording from untreated/control neurons for the first 2-3 hours.

Recording of Spontaneous Network Activity.

For monitoring Spontaneous Network Activity (SNA), tight-fitting glass suction electrodes were used to record ventrolateral Funiculus (VLF) signals as described previously (O'Donovan and Landmesser, 1987). VLF signals were amplified (1000X), filtered (0.1 Hz to 1 kHz) by an extracellular amplifier (A-M Systems Inc.) and acquired using PClamp 10 (Molecular Devices). Analyses of the data were performed offline.

Immunoblots.

The ventral half of the lumbosacral spinal cords were homogenized in RIPA buffer containing protease and phosphatase inhibitors. Samples were then centrifuged to remove cell debris. Protein concentration was quantitated using BCA reagent (Pierce). Samples were separated on 4–15% SDS-PAGE and blotted to a nitrocellulose membrane. Films were scanned and analyzed using free software, ImageJ, with background correction and normalization to actin. The primary antibodies against Nav 1.2 and Kv 4.2 were from Alomone Labs. The blots were visualized by ECL chemiluminescence (GE Healthcare). Lysate from the ventral half of 4 different cords/chicks per treatment were used and blots were done in duplicate (total 8 embryos per treatment).

Drugs.

SR-95531 hydrobromide (gabazine), 6-Cyano-7-nitroquinoxaline-2,3-dione disodium (CNQX), D-(-)-2-Amino-5-phosphonopentanoic acid (APV), and Dihydro-β-erythroidine hydrobromide (DHβE) were purchased from Tocris Cookson (Cat. No. 1262, Cat. No. 1045, Cat. No. 0106, and Cat. No. 2349 respectively); All other chemicals and drugs were purchased from Sigma-Aldrich.

Statistics.

Data are expressed as mean ± SE. Statistical analysis of cellular excitability parameters was performed using ANOVA followed by Bonferroni post hoc test for multiple comparisons for normally distributed data and Kruskal-Wallis method followed by a post-hoc Dunn test for data that was not normally distributed, unless mentioned otherwise. For statistical assessment of mPSC amplitude we used a student t-test for normally distributed data, and Mann-Whitney test for data that was not normally distributed. For all of the experiments the number of cells and cords are indicated in parenthesis at the bottom of the corresponding figure legend. Throughout the manuscript * refers to $p \leq 0.05$, ** refers to $p \leq 0.01$, and *** refers to $p \leq 0.001$.

Results.

Changes in spinal neuron excitability in the first 12 hours of in vivo GABAergic blockade.

Previous work showed that spinal motoneuron voltage-gated Na^+ and K^+ channel currents were altered following 12 hours of *in ovo* GABAergic blockade, after embryonic movements had homeostatically recovered (Wilhelm et al., 2009). In order to determine if these changes actually contribute to the recovery, we assessed cellular excitability in motoneurons during the period that the SNA-driven movements were actually recovering, but before complete recovery was achieved. First, we tested whether cellular excitability had increased during the period that movements were in the process of homeostatically recovering, following 6 hours of gabazine treatment (10μM) *in ovo*. We isolated the spinal cord following saline/gabazine treatment and recorded whole cell in current clamp from motoneurons that were no longer in the presence of gabazine. We found that threshold current (rheobase) was reduced and the absolute threshold voltage was hyperpolarized suggesting the cells were more excitable following 6 hours of gabazine treatment (Figure 1B, C, Table 1). Following 12 hours of gabazine treatment *in ovo* similar changes were observed (Figure 1B, C, Table 1). We also assessed excitability by giving current steps and plotting this against firing frequency after either 6 or 12 hours of gabazine treatment (Figure 1A). We saw a very strong shift toward higher excitability in the F-I curve at the 6 hour time point, which then moved partly back toward pre-drug values following 12 hour treatment, although cells still showed a heightened excitability compared to controls. We did not observe changes in resting membrane potential or input resistance (Figure 1D, E).

We wanted to determine whether these increases in cellular excitability were only occurring in motoneurons, or whether this was a more general phenomenon that extends to the rest of the developing motor circuitry. Thus, we assessed the possibility that spinal interneurons also increased cell excitability following gabazine treatment and could therefore contribute to the homeostatic recovery of SNA. Spinal neurons were targeted in the more medial positions of the cord. The population of spinal interneurons we recorded from were targeted blindly and therefore represent a diverse class of spinal interneurons with different neurotransmitters and activity patterns (Ritter et al., 1999). We found that, like motoneurons, interneurons had reduced threshold current at 6 and 12 hours of gabazine treatment (Figure 2B, Table 1). Threshold voltage was hyperpolarized at 12 hours of gabazine treatment (Figure 2C, Table 1). In addition, we did see a depolarization of the RMP at 6 hours of treatment (Figure 2D). Overall the results suggest that there were increases in intrinsic excitability in motoneurons and interneurons at the point that embryonic movements were homeostatically recovering from *in ovo* $GABA_A$ receptor blockade.

Changes in spinal neuron excitability in the first 6 hours of in vitro GABAergic blockade.

One advantage of the earlier experiments was that the perturbation was carried out *in vivo*. Unfortunately, in order to measure cellular excitability the cord must be isolated and was given several hours to recover in the absence of gabazine before we could make excitability measurements. Such a process could itself alter the excitability of the cells. Therefore, in addition to the *in vivo* perturbations, we wanted to assess

306 cellular excitability changes in the isolated cord *in vitro* in the first 6 hours after adding
307 the $GABA_A$ receptor antagonist gabazine (10μM). First, we added gabazine to the bath
308 and observed its effect on the expression of SNA. Similar to previous work, we saw that
309 episodes of SNA were initially blocked, but then began to recover in the following hours
310 of GABAergic blockade (Figure 3). As reported previously (Chub and O'Donovan,
311 1998), the duration of the episodes of SNA was reduced following bath addition of
312 gabazine (Figure 3 - 1). To identify the mechanisms that recover SNA and which are
313 expressed in the continued presence of gabazine we recorded whole cell in current
314 clamp from motoneurons in the first (0-2), second (2-4), third (4-6) two hour periods,
315 and in cells that were never exposed to gabazine. Several aspects of cellular
316 excitability were observed to increase in these first 6 hours of GABAergic block. We saw
317 a reduced threshold current (2-6 hours, Figure 4B1, Table 1), a hyperpolarized
318 threshold voltage (0-2 & 4-6 hours, Figure 4B2, Table 1), and importantly, a fast ~10mV
319 depolarization of the RMP (0-6 hours, Figure 4B3, Table 1). Cords that were never
320 treated with gabazine *in vitro* but where motoneurons were recorded from 0-2 hours, 2-4
321 hours, or 4-6 hours after warming the bath showed that the depolarized RMP was not
322 simply a time-dependent process (Figure 4B3 inset). Interestingly, we did not see a
323 significant change in input resistance (Figure 4B4, Table 1). These results suggest that
324 compensatory changes in motoneuron excitability occurs very quickly and therefore
325 could contribute to the recovery of SNA. The most striking compensatory change was a
326 depolarizing shift in the RMP.

327 Similar increases in cellular excitability were observed in interneurons from
328 isolated cords that were treated with bath application of gabazine for 0-2, 2-4, and 4-

6hrs *in vitro* (Figure 4D1-4, Table 1). Cords that were never treated with gabazine but where interneurons were recorded from 0-2 hours, 2-4 hours, or 4-6 hours after warming the bath showed that the depolarized RMP was not simply a time-dependent process (Figure 4 D3 inset). Because we were recording from diverse classes of spinal neurons, the results suggest that various cell types alter their cellular intrinsic excitability and contribute to the recovery of activity following GABAergic blockade. Importantly, interneuron RMP was significantly depolarized at each of the time points (Figure 4D3). No changes were observed in input resistance in any condition. Therefore, interneurons increased their cellular excitability after GABAergic blockade similarly to motoneurons.

Since the changes in cellular excitability following $GABA_AR$ blockade appear to be expressed across multiple cell types throughout much of the cord, we ran Western blots of isolated spinal cords (ventral half) and assessed 2 of the voltage-gated channels that we expected could mediate this process. It has been reported (Wilhelm et al., 2009) that gabazine-induced changes were observed in voltage-gated Na^+ and K^+ channels. In that study we saw TTX-sensitive voltage-gated Na^+ channel currents were increased. Therefore, we assessed the levels of Nav1.2, an alpha subunit of the voltage-gated Na^+ channel, which had been shown to be expressed early in the development of the embryonic chick (Kuba et al., 2014). We found that following 12 hour gabazine treatment *in ovo*, Nav1.2 expression was increased (172.4±14.8%, $p \leq 0.05$), but not after 6 hour treatment (105.3 ± 5.3%, Figure 5). Further, it was also observed in that study that currents of the A-type transiently-activated K^+ channel (I_A) and the calcium-dependent K^+ channel ($I_{K(Ca)}$) were both decreased following gabazine treatment (Wilhelm et al., 2009). Here, we show that expression of Kv4.2 (mediates the

352 A-type K^+ channel in chick embryo (Dryer et al., 1998)) is down regulated following 12
353 hour gabazine treatment (54.5 ± 2.5%, $p \leq 0.05$), but not after 6 hours (104.2 ± 17.2%,
354 Figure 5). Together the results show that cellular excitability is altered during and after
355 the homeostatic recovery of SNA, and that expression changes in two different voltage-
356 gated channels do not occur until later stages of the recovery.
357
358 **The trigger for changes in RMP was distinct from the homeostatic mechanisms**
359 **expressed after GABAergic blockade.**
360 Following GABAR blockade compensatory changes in synaptic strength (scaling)
361 were not observed until 48 hours, but voltage-gated conductance changes were
362 triggered by 12 hours (Wilhelm and Wenner, 2008; Wilhelm et al., 2009). It has been
363 recently reported that simply reducing $GABA_AR$ activation due to spontaneous miniature
364 release of GABA vesicles (spontaneous GABAergic transmission) was sufficient to
365 trigger upscaling (Garcia-Bereguiain et al., 2016). We were able to do this by taking
366 advantage of our observation that manipulating nicotinic receptor activation altered
367 spontaneous GABAergic release (Gonzalez-Islas et al., 2016). In this previous study we
368 showed that the nicotinic antagonist DHβE, reduces $GABA_A$, but not AMPA, mPSCs by
369 ~30%. Therefore, we tested the possibility that the fast changes in cellular excitability
370 observed in the current study were also mediated by reduced spontaneous miniature
371 GABAergic neurotransmission. Whole cell recordings from motoneurons were obtained
372 before and 2 hours after DHβE application *in vitro*. We did not find any differences in
373 cellular excitability following reduction of GABA quantal release by DHβE (Figure 6).
374 Therefore, unlike the trigger for synaptic scaling, the compensatory changes in cellular

375 excitability in the first hours of GABAergic blockade were not mediated by changes in
376 spontaneous GABAergic transmission.
377
378 ***Synaptic scaling does not contribute to the homeostatic recovery of SNA-***
379 ***generated movements.***
380 Previously, it had been shown that AMPAergic and GABAergic upscaling were
381 not observed in chick embryo motoneurons following 12 hour gabazine treatment *in ovo*
382 (Wilhelm and Wenner, 2008). It remained possible that interneurons experienced
383 scaling and contributed to the homeostatic recovery of SNA in the first hours of
384 gabazine treatment. However, following 6hrs of gabazine treatment *in ovo* we found no
385 change in interneurons in AMPA mPSC amplitude (Figure 7A) or decay kinetics (Figure
386 7 - 1). We would not have expected GABAergic scaling to contribute to the recovery of
387 movements as we were blocking $GABA_A$ receptors. Regardless, we did not see any
388 change in GABA mPSC amplitude (Figure 7A) or decay kinetics (Figure 7 - 1) in
389 interneurons following 6hr gabazine treatment *in ovo*. The results show that neither
390 AMPAergic nor GABAergic scaling in interneurons contributed to the homeostatic
391 recovery of activity levels.
392 It was shown previously that scaling is not triggered in motoneurons after 12
393 hours of gabazine treatment (Wilhelm and Wenner, 2008). We tested whether
394 AMPAergic and GABAergic scaling was expressed in motoneurons following 6 hours of
395 gabazine treatment *in ovo*. We found no difference in AMPAergic or GABAergic mPSC
396 amplitude (Figure 7C) or decay kinetics (Figure 7 - 1) from controls. These findings
397 showed that synaptic scaling of AMPAergic mPSCs in different spinal populations could

not have contributed to the recovery of SNA or the movements it drives following GABAergic blockade. Finally, there was no compensatory increase in mPSC frequency in interneurons (Figure 7B), or motoneurons (Figure 7D). In fact, we found a significant reduction in GABAergic mPSC frequency.

Recovery of embryonic movements following glutamatergic blockade is mediated by fast changes in resting membrane potential.

Previous work has demonstrated that a similar homeostatic recovery of embryonic movements was observed following either glutamatergic or GABAergic blockade (Wilhelm and Wenner, 2008). Movements recovered in around 12 hours, but after 12 hours of glutamatergic blockade no synaptic scaling or homeostatic changes in intrinsic excitability were observed. However, it is unknown if changes in intrinsic excitability occur at earlier time points in the presence of glutamatergic antagonists. Therefore, we isolated spinal cords and applied CNQX (20μM)/APV (50μM) to the *in vitro* preparation and monitored the expression of SNA. We saw that glutamatergic blockade delayed the next episode of activity but then recovered to a slightly faster rate than before the drugs were added (Figure 8). As reported previously (Chub and O'Donovan, 1998), the duration of the episodes of SNA was reduced following bath addition of CNQX/APV (Figure 8 - 1). We examined the compensatory changes in intrinsic excitability that might mediate the increased excitability of these cords. We assessed intrinsic excitability from 0-6 hours of glutamate receptor blockade in the continued presence of the antagonists. We observed that motoneurons did indeed express reductions in threshold current from 2-6 hours and a hyperpolarized threshold

voltage at 4-6 hours of drug application (Figure 9B-C, Table 1). In addition, there was a significant depolarization of resting membrane potential (>10mV) from 0-6 hours accompanied by no change in input resistance from 0-4 hours (Figure 9D-E, Table 1). Similar changes were observed in interneurons following glutamatergic blockade, however the compensations in threshold voltage and RMP (>15mV) were even more dramatic, while threshold voltage was slightly hyperpolarized but this did not reach significance (Figure 10, Table 1). The results suggest fast homeostatic changes in membrane potential significantly contribute to compensatory changes triggered by neurotransmitter receptor blockade. Together, the results focus our attention on homeostatic changes in RMP as contributors to the recovery of embryonic movements during either GABAergic or glutamatergic blockade.

Discussion

Homeostatic mechanisms such as synaptic scaling and changes in voltage-gated conductances are thought to be the main strategies that allow maintenance of activity levels. Here we describe a new mechanism for homeostatic recovery using compensatory changes in RMP that occurs in the first hours of the perturbation.

Homeostatic mechanisms and their contribution to the recovery of embryonic activity following neurotransmitter receptor blockade.

Synaptic scaling was not expressed at 6 hours in motoneurons or interneurons (Figure 7), and therefore this form of homeostatic plasticity does not appear to be

444 involved in the recovery of embryonic spinal activity, consistent with previous work
445 (Wilhelm and Wenner, 2008). While scaling does not appear to mediate the recovery in
446 the embryonic spinal cord, it appears to influence recovery of spiking activity in the
447 cortex following *in vivo* sensory deprivation (Hengen et al., 2013; Glazewski et al.,
448 2017), however see (Bridi et al., 2018).

449 Compensatory changes in homeostatic intrinsic excitability were observed
450 following 6 and 12 hours of *in vivo* GABAergic blockade. Significant reductions in
451 threshold current were observed in both motoneurons and interneurons. This appears to
452 be largely due to a hyperpolarization of the threshold voltage. On the other hand,
453 compensatory changes in RMP were not observed, with one exception (interneurons
454 following 6 hour gabazine treatment). Therefore, $GABA_A$ receptor blockade *in vivo*
455 triggers clear compensatory changes in threshold voltage at both 6 and 12 hours of
456 treatment that can be observed in the isolated cord no longer in the presence of the
457 GABAergic antagonist.

458

459 These mechanisms were different when the cord was treated with GABAergic or
460 glutamatergic receptor antagonists *in vitro*, where the drugs remained in place as we
461 made measurements of cellular excitability. We observed some changes in threshold
462 voltage in motoneurons and interneurons, but it was clear that reductions in threshold
463 current were, in this case, largely due to significant depolarizations in RMP (>10mV), at
464 0-2, 2-4, and 4-6 hours of GABAergic or glutamatergic blockade in both motoneurons
465 and interneurons. The recovery of embryonic movements following GABAergic and
466 glutamatergic blockade were temporally very similar, even though the mechanisms

467 appeared to be distinct as compensatory changes in threshold current were not
468 previously observed following 12 hour glutamatergic blockade *in ovo* (Wilhelm et al.,
469 2009). This, therefore, focusses our attention on the fast homeostatic changes in RMP
470 as a critical mechanism of homeostatic recovery of SNA in this developing circuitry.
471 The spinal interneurons were patched blindly, and so this population will
472 represent a diverse one of many cell classes (Ritter et al., 1999). Therefore, in cases
473 where we did not see a change in the measured parameter, the variability of the
474 populations could contribute to this. Similarly, we did not distinguish among
475 motoneurons projecting to different muscles, and so again this could contribute to
476 variability. Importantly, no matter what kind of interneuron (GABAergic or glutamatergic)
477 or motoneuron (femorotibialis or tibialis anterior) that we recorded from, the change in
478 resting membrane potential was a universally observed feature. Further, it is becoming
479 clear that variability is a biological reality as functionally equivalent cells and circuits can
480 achieve their common behaviors using highly different strategies or parameter space
481 solutions (distinct constellations of synaptic and voltage gated conductances) (Marder et
482 al., 2015).
483
484 **Homeostatic perturbations and RMP**
485 No changes in RMP were reported in two of the earliest studies on homeostatic
486 plasticity where different strategies were used to chronically block spiking for days (TTX,
487 CNQX, or cell isolation) - in rat cortical cultures (Turrigiano et al., 1998) or the
488 stomatogastric neurons of the lobster (Turrigiano et al., 1994). Since these early
489 studies, several other homeostatic experiments have been performed where spiking or

490 neurotransmission were chronically blocked to trigger homeostatic synaptic or intrinsic
491 plasticity and no changes in RMP were observed. These studies have been carried out
492 using various perturbations (TTX, TTX/APV, CNQX, NBQX, gabazine, bicuculline, cell
493 isolation) in rat cortical cultures (Turrigiano et al., 1998), mouse cortical cultures (Bülow
494 et al., 2019), and in the embryonic spinal cord of the chick embryo *in* vivo (Gonzalez-
495 Islas and Wenner, 2006; Wilhelm and Wenner, 2008; Wilhelm et al., 2009). On the other
496 hand, none of these studies followed the RMP before and immediately after the
497 perturbation as we have done in the current study. Therefore, changes in RMP may
498 have occurred in these previous studies but over the duration and/or after removal of
499 the perturbation no change was detected. An exception to this was described following
500 a strong perturbation (2 week exposure to 15mM KCl), where a homeostatic
501 hyperpolarization of RMP was observed in cultured hippocampal neurons (O'Leary et
502 al., 2010).
503
504 **Conductances that contribute to the RMP.**
505 Several different ion channels exhibit activation at subthreshold potentials and
506 thus contribute to setting the RMP including multiple kinds of K^+ channels (Ia, Ikir, Ileak)
507 (Plant et al.; Coetzee et al., 1999), hyperpolarization-activated cationic channels (Ih)
508 (Robinson and Siegelbaum, 2003; Biel et al., 2009), low-threshold calcium channels
509 (Perez-Reyes, 2003), persistent sodium currents (NaPIC) (Crill, 1996; Waxman et al.,
510 2002), and leak sodium channels (NALCN) (Lu et al., 2007; Ren, 2011). In addition,
511 ongoing synaptic conductances can also influence the RMP (Mody and Pearce, 2004;
512 Chuang and Reddy, 2018). Previous work has shown that blocking GABARs by direct

application of a GABA receptor antagonist onto a chick embryo spinal cord preparation causes an acute hyperpolarization in spinal neurons that can be as large as 10mV, suggesting a significant tonic GABAergic depolarizing current (Chub and O'Donovan, 2001). The effect of acute application of GABAergic antagonist onto the cord (Chub and O'Donovan, 2001) is in the opposite direction (hyperpolarizing) compared to the current studies finding that bath application of gabazine leads to a depolarization of RMP in the first hours of drug exposure. The current study is the only one we are aware of that follows RMP before and throughout the first hours of the perturbation and may explain why this form of homeostatic intrinsic plasticity has not been previously reported.

Mechanisms of early homeostatic changes following neurotransmitter receptor blockade.

What is a potential trigger for these homeostatic changes in RMP? It has been shown previously that homeostatic synaptic scaling is triggered following 48 hour block of GABAergic transmission (Wilhelm and Wenner, 2008) and compensatory changes in voltage-gated ion channel conductances by 12 hours of GABAR block (Wilhelm et al., 2009). In fact, merely altering GABAR activation due to spontaneous release of GABA vesicles can fully trigger synaptic scaling (Garcia-Bereguiain et al., 2016). However, compensatory changes in RMP were not so reliant on GABAR activation. Fast changes in RMP were not triggered by altering the frequency of spontaneous vesicle-mediated GABAR activation (Figure 6). Further, these changes can also be triggered by reduced glutamatergic receptor activation where GABAR activation is intact. Therefore, the most straightforward explanation for the trigger of homeostatic changes in RMP would be the

536 reduction in network activity caused by blocking either glutamatergic or GABAergic
537 receptors.
538
539 A commonly described mechanism underlying a change in RMP involves a
540 change in some resting channel conductance (e.g. K^+ channels), however we did not
541 detect a change in input resistance, making this possibility less likely. A potentially more
542 plausible mechanism would involve a change in the function of the Na^+/K^+ ATPase.
543 Previous studies are consistent with this possibility. First, resting membrane potential of
544 invertebrate neurons can be changed by an alteration of the electrogenic Na^+/K^+
545 ATPase (Carpenter and Alving, 1968; Carpenter, 1973; Willis et al., 1974). Next, work in
546 the spinal cord of xenopus and neonatal mice, as well as in motoneurons of the fly
547 larva, show that bursts of spiking activity expressed in these systems lead to an
548 increase in intracellular Na^+, that is necessary to activate an isoform of the Na^+/K^+
549 ATPase that is not active at baseline Na^+ levels. The Na^+-dependent activation of this
550 Na^+/K^+ ATPase produces a hyperpolarizing current due to the electrogenic nature of the
551 pump that has been called an ultra slow afterhyperpolarization (usAHP) (Pulver and
552 Griffith, 2010; Zhang and Sillar, 2012; Picton et al., 2017b; Picton et al., 2017a). This
553 hyperpolarizing current is maintained for up to a minute. SNA in the chick embryo spinal
554 preparation experiences a very similar usAHP after episodes of SNA (O'Donovan, 1999;
555 Chub and O'Donovan, 2001). Further, embryonic spinal neurons have very high Na^+
556 concentrations at baseline (Lindsly et al., 2017). Therefore, it is possible that Na^+ levels
557 constitutively activate this Na^+/K^+ ATPase and when SNA is blocked for many minutes
558 by glutamatergic or GABAergic antagonists, Na^+ levels eventually are reduced to a point

559 that pump activity is minimized and the hyperpolarizing current abates, thus
560 depolarizing the RMP.
561
562 Most of our results appear to suggest that the changes in RMP are expressed
563 transiently while the antagonists are in place, and once washed off the RMP returns to
564 pre-drug levels. This kind of temporary perturbation might not permanently change the
565 developmental trajectory of spinal neurons or their network. However, if this initial fast
566 homeostatic mechanism does not recover activity levels or is maintained for long
567 periods, then other mechanisms may be triggered, which could alter the development of
568 the spinal circuitry in a long lasting manner. This may be the case following GABAergic
569 blockade where compensatory changes in threshold voltage are triggered *in vivo* and *in*
570 *vitro*. This is consistent with previous 12 hour GABAergic blockade *in vivo* where
571 threshold current is dramatically reduced by compensatory changes in voltage-gated
572 Na^+ and K+ channels (Wilhelm et al., 2009). Changes in protein levels of 2 of these
573 previously implicated voltage-gated ion channels were observed at 12 hours, although
574 not at 6 hours of *in vivo* gabazine treatment (Figure 5). In some cases, homeostatic
575 changes in RMP may be sufficient and exist temporarily, but in other cases these
576 additional mechanisms could be engaged to recover the activity.
577
578
579
580
581

582
583
584
585
586
587
588

589 **Bibliography**

590 Barry MJ, O'Donovan MJ (1987) The effects of excitatory amino acids and their antagonists
591 on the generation of motor activity in the isolated chick spinal cord. Brain Res
592 433:271-276.
593 Ben-Ari Y, Cherubini E, Corradetti R, Gaiarsa JL (1989) Giant synaptic potentials in
594 immature rat CA3 hippocampal neurones. J Physiol (Lond) 416:303-325.
595 Biel M, Wahl-Schott C, Michalakis S, Zong X (2009) Hyperpolarization-activated cation
596 channels: from genes to function. Physiol Rev 89:847-885.
597 Blankenship AG, Feller MB (2010) Mechanisms underlying spontaneous patterned activity
598 in developing neural circuits. Nat Rev Neurosci 11:18-29.
599 Bridi MCD, de Pasquale R, Lantz CL, Gu Y, Borrell A, Choi SY, He K, Tran T, Hong SZ, Dykman
600 A, Lee HK, Quinlan EM, Kirkwood A (2018) Two distinct mechanisms for experience-
601 dependent homeostasis. Nat Neurosci 21:843-850.
602 Bülow P, Murphy TJ, Bassell GJ, Wenner P (2019) Homeostatic Intrinsic Plasticity Is
603 Functionally Altered in Fmr1 KO Cortical Neurons. Cell Rep 26:1378-1388 e1373.
604 Carpenter DO (1973) Electrogenic sodium pump and high specific resistance in nerve cell
605 bodies of the squid. Science 179:1336-1338.
606 Carpenter DO, Alving BO (1968) A contribution of an electrogenic Na+ pump to membrane
607 potential in Aplysia neurons. J Gen Physiol 52:1-21.
608 Chuang SH, Reddy DS (2018) Genetic and Molecular Regulation of Extrasynaptic GABA-A
609 Receptors in the Brain: Therapeutic Insights for Epilepsy. J Pharmacol Exp Ther
610 364:180-197.
611 Chub N, O'Donovan MJ (1998) Blockade and recovery of spontaneous rhythmic activity
612 after application of neurotransmitter antagonists to spinal networks of the chick
613 embryo. J Neurosci 18:294-306.
614 Chub N, O'Donovan MJ (2001) Post-episode depression of GABAergic transmission in spinal
615 neurons of the chick embryo. J Neurophysiol 85:2166-2176.
616 Coetzee WA, Amarillo Y, Chiu J, Chow A, Lau D, McCormack T, Moreno H, Nadal MS, Ozaita
617 A, Pountney D, Saganich M, Vega-Saenz de Miera E, Rudy B (1999) Molecular
618 diversity of K+ channels. Ann N Y Acad Sci 868:233-285.

619 Crill WE (1996) Persistent sodium current in mammalian central neurons. Annu Rev
620 Physiol 58:349-362.
621 Davis GW (2013) Homeostatic signaling and the stabilization of neural function. Neuron
622 80:718-728.
623 Desai NS, Cudmore RH, Nelson SB, Turrigiano GG (2002) Critical periods for experience-
624 dependent synaptic scaling in visual cortex. Nat Neurosci 5:783-789.
625 Dryer L, Xu Z, Dryer SE (1998) Arachidonic acid-sensitive A-currents and multiple Kv4
626 transcripts are expressed in chick ciliary ganglion neurons. Brain Res 789:162-166.
627 Echegoyen J, Neu A, Graber KD, Soltesz I (2007) Homeostatic plasticity studied using in
628 vivo hippocampal activity-blockade: synaptic scaling, intrinsic plasticity and age-
629 dependence. PLoS One 2:e700.
630 Garcia-Bereguiain MA, Gonzalez-Islas C, Lindsly C, Wenner P (2016) Spontaneous Release
631 Regulates Synaptic Scaling in the Embryonic Spinal Network In Vivo. J Neurosci
632 36:7268-7282.
633 Glazewski S, Greenhill S, Fox K (2017) Time-course and mechanisms of homeostatic
634 plasticity in layers 2/3 and 5 of the barrel cortex. Philos Trans R Soc Lond B Biol Sci
635 372.
636 Goel A, Jiang B, Xu LW, Song L, Kirkwood A, Lee HK (2006) Cross-modal regulation of
637 synaptic AMPA receptors in primary sensory cortices by visual experience. Nat
638 Neurosci 9:1001-1003.
639 Gonzalez-Islas C, Wenner P (2006) Spontaneous Network Activity in the Embryonic Spinal
640 Cord Regulates AMPAergic and GABAergic Synaptic Strength. Neuron 49:563-575.
641 Gonzalez-Islas C, Garcia-Bereguiain MA, O'Flaherty B, Wenner P (2016) Tonic nicotinic
642 transmission enhances spinal GABAergic presynaptic release and the frequency of
643 spontaneous network activity. Dev Neurobiol 76:298-312.
644 Hall BK, Herring SW (1990) Paralysis and growth of the musculoskeletal system in the
645 embryonic chick. J Morphol 206:45-56.
646 Hamburger V, Hamilton HL (1951) A series of normal stages in the development of the
647 normal chick embryo. J Morphol 88:49-92.
648 Hanson MG, Landmesser LT (2004) Normal patterns of spontaneous activity are required
649 for correct motor axon guidance and the expression of specific guidance molecules.
650 Neuron 43:687-701.
651 Hengen KB, Lambo ME, Van Hooser SD, Katz DB, Turrigiano GG (2013) Firing rate
652 homeostasis in visual cortex of freely behaving rodents. Neuron 80:335-342.
653 Jarvis JC, Sutherland H, Mayne CN, Gilroy SJ, Salmons S (1996) Induction of a fast-oxidative
654 phenotype by chronic muscle stimulation: mechanical and biochemical studies. Am J
655 Physiol 270:C306-312.
656 Knogler LD, Liao M, Drapeau P (2010) Synaptic scaling and the development of a motor
657 network. J Neurosci 30:8871-8881.
658 Kuba H, Oichi Y, Ohmori H (2010) Presynaptic activity regulates Na(+) channel distribution
659 at the axon initial segment. Nature 465:1075-1078.
660 Kuba H, Adachi R, Ohmori H (2014) Activity-dependent and activity-independent
661 development of the axon initial segment. J Neurosci 34:3443-3453.
662 Lindsly C, Gonzalez-Islas C, Wenner P (2017) Elevated intracellular Na(+) concentrations in
663 developing spinal neurons. J Neurochem 140:755-765.

664 Lu B, Su Y, Das S, Liu J, Xia J, Ren D (2007) The neuronal channel NALCN contributes resting
665 sodium permeability and is required for normal respiratory rhythm. Cell 129:371-
666 383.
667 Marder E, Goaillard JM (2006) Variability, compensation and homeostasis in neuron and
668 network function. Nat Rev Neurosci 7:563-574.
669 Marder E, Goeritz ML, Otopalik AG (2015) Robust circuit rhythms in small circuits arise
670 from variable circuit components and mechanisms. Curr Opin Neurobiol 31:156-
671 163.
672 Mody I, Pearce RA (2004) Diversity of inhibitory neurotransmission through GABA(A)
673 receptors. Trends Neurosci 27:569-575.
674 Neher E (1992) Correction for liquid junction potentials in patch clamp experiments.
675 Methods Enzymol 207:123-131.
676 O'Donovan MJ (1999) The origin of spontaneous activity in developing networks of the
677 vertebrate nervous system. Curr Opin Neurobiol 9:94-104.
678 O'Donovan MJ, Landmesser L (1987) The development of hindlimb motor activity studied
679 in the isolated spinal cord of the chick embryo. J Neurosci 7:3256-3264.
680 O'Donovan MJ, Chub N, Wenner P (1998) Mechanisms of spontaneous activity in
681 developing spinal networks. J Neurobiol 37:131-145.
682 O'Leary T, van Rossum MC, Wyllie DJ (2010) Homeostasis of intrinsic excitability in
683 hippocampal neurones: dynamics and mechanism of the response to chronic
684 depolarization. J Physiol 588:157-170.
685 Perez-Reyes E (2003) Molecular physiology of low-voltage-activated t-type calcium
686 channels. Physiol Rev 83:117-161.
687 Persson M (1983) The role of movements in the development of sutural and diarthrodial
688 joints tested by long-term paralysis of chick embryos. J Anat 137:591-599.
689 Picton LD, Zhang H, Sillar KT (2017a) Sodium pump regulation of locomotor control
690 circuits. J Neurophysiol 118:1070-1081.
691 Picton LD, Nascimento F, Broadhead MJ, Sillar KT, Miles GB (2017b) Sodium Pumps
692 Mediate Activity-Dependent Changes in Mammalian Motor Networks. J Neurosci
693 37:906-921.
694 Plant LD, Bayliss DA, Minor DL, CZzirjak G, Enyedi P, Lesage F, Sepulveda F, Golsdstein SA
695 Two P domain potassium channels. IUPHAR/BPS Guide to PHARMACOLOGY.
696 Pulver SR, Griffith LC (2010) Spike integration and cellular memory in a rhythmic network
697 from Na+/K+ pump current dynamics. Nat Neurosci 13:53-59.
698 Ren D (2011) Sodium leak channels in neuronal excitability and rhythmic behaviors.
699 Neuron 72:899-911.
700 Ritter A, Wenner P, Ho S, Whelan P, O'Donovan MJ (1999) Activity patterns and synaptic
701 organization of ventrally located interneurons in the embryonic chick spinal cord. J
702 Neurosci 19:3457-3471.
703 Rivera C, Voipio J, Payne JA, Ruusuvuori E, Lahtinen H, Lamsa K, Pirvola U, Saarma M, Kaila
704 K (1999) The K+/Cl- co-transporter KCC2 renders GABA hyperpolarizing during
705 neuronal maturation. Nature 397:251-255.
706 Robinson RB, Siegelbaum SA (2003) Hyperpolarization-activated cation currents: from
707 molecules to physiological function. Annu Rev Physiol 65:453-480.
708 Roufa D, Martonosi AN (1981) Effect of curare on the development of chicken embryo
709 skeletal muscle in ovo. Biochem Pharmacol 30:1501-1505.

Ruano-Gil D, Nardi-Vilardaga J, Tejedo-Mateu A (1978) Influence of extrinsic factors on the development of the articular system. Acta Anat (Basel) 101:36-44.

Toutant JP, Toutant MN, Renaud D, Le Douarin GH (1979) Enzymatic differentiation of muscle fibre types in embryonic latissimus dorsii of the chick: effects of spinal cord stimulation. Cell Differ 8:375-382.

Turrigiano G (2011) Too many cooks? Intrinsic and synaptic homeostatic mechanisms in cortical circuit refinement. Annu Rev Neurosci 34:89-103.

Turrigiano G, Abbott LF, Marder E (1994) Activity-dependent changes in the intrinsic properties of cultured neurons. Science 264:974-977.

Turrigiano GG, Leslie KR, Desai NS, Rutherford LC, Nelson SB (1998) Activity-dependent scaling of quantal amplitude in neocortical neurons. Nature 391:892-896.

Waxman SG, Cummins TR, Black JA, Dib-Hajj S (2002) Diverse functions and dynamic expression of neuronal sodium channels. Novartis Found Symp 241:34-51; discussion 51-60.

Wilhelm JC, Wenner P (2008) GABAA transmission is a critical step in the process of triggering homeostatic increases in quantal amplitude. Proc Natl Acad Sci U S A 105:11412-11417.

Wilhelm JC, Rich MM, Wenner P (2009) Compensatory changes in cellular excitability, not synaptic scaling, contribute to homeostatic recovery of embryonic network activity. Proc Natl Acad Sci U S A 106:6760-6765.

Willis JA, Gaubatz GL, Carpenter DO (1974) The role of the electrogenic sodium pump in modulation of pacemaker discharge of Aplysia neurons. J Cell Physiol 84:463-472.

Zhang HY, Sillar KT (2012) Short-term memory of motor network performance via activity-dependent potentiation of Na+/K+ pump function. Curr Biol 22:526-531.

Figure Legends

Figure 1. Changes in motoneuron excitability observed after chronic *in vivo* gabazine treatments. Motoneuron excitability was measured in isolated embryonic spinal cords by whole cell current clamp using progressively more depolarized current steps to assess rheobase current and voltage threshold. Measurements were obtained from embryos that were untreated (12 cells, 5 cords), or treated for 6 (7 cells, 4 cords) or 12 (9 cells, 5 cords) hours with gabazine (10μM at E9.5 or E9.75). **(A)** Average F-I curves for control motoneurons (n=9), 6 hr gabazine treatment (n=6) or 12 hr gabazine treatment (n=9). Gabazine treatments shifted the average F-I curve to the left. All curves were significantly different from each other (values for steps of 90-110pAs were combined, horizontal bar, one way ANOVA, Tukey post $p<0.001$). The arrows point to representative traces for each condition evoked by current steps of 100 pA. Threshold current (**B**) or threshold voltage (**C)** was obtained by determining the minimum current necessary to evoke a spike in the recorded motoneuron. No significant changes in resting membrane potential **(D**) or Input resistance (**E**) were found in the motoneurons

768 recorded after chronic gabazine treatment at 6 or 12 hrs. * P<0.05; ** P<0.01 and
769 ***P<0.001.
770
771 **Figure 2. Interneuron excitability increased following *in vivo* GABAergic**
772 **blockade.** Interneuron excitability was measured in isolated spinal cords from control or
773 after *in ovo* chronic treatment with gabazine (10μM) for 6 or 12 hours. A step protocol
774 (1s, in 1pA increments) was used to assess rheobase current and voltage threshold.
775 Representative traces of interneuron firing in control (10 cells, 5 cords), or after 6 (12
776 cells, 4 cords) and 12 (n=9, 3 cords) hours of chronic *in ovo* treatment with gabazine.
777 Under each trace, the corresponding rheobase current applied to evoke firing is shown.
778 Resting membrane potential (RMP) is also indicated at the left of each trace. Box and
779 whisker plots superimposed to their corresponding dot plots show quartile distribution
780 and individual values for Rheobase (**B**), spike threshold voltage (**C**), resting membrane
781 potential (**D**), and input resistance (**E**). Kruskal-Wallis method followed by a post-hoc
782 Dunn test was used to assess statistical significance. ** P<0.01 and ***P<0.001. For all
783 plots, the continuous line represents the median and the dotted line represent the mean
784 of the sample.
785
786 **Figure 3. Episodes of spontaneous network activity are abolished and then begin**
787 **to recover following GABAergic blockade.** The interval between episodes of SNA
788 are plotted against elapsed time for 3 different cords before and following addition of
789 gabazine to the bath. Episode intervals were increased following GABAergic block
790 (10μM gabazine), but then began to recover in the hours following gabazine. Inset

791 shows example traces of SNA from a cord before (black) and after bath addition of
792 gabazine (grey). Traces were filtered from 0.1Hz – 10KHz.
793
794 **Figure 4. Spinal neuron excitability increased during the continuous blockade of**
795 **$GABA_A$ receptors *in vitro*.** Motoneuron excitability was measured in isolated spinal
796 cords using a ramp protocol from 0 to 200 pA in 1.2 sec to assess rheobase current and
797 voltage threshold in the absence (control – 33 cells, 12 cords) or in the continuous
798 presence of gabazine 10 mM at 3 different blockade periods: 0-2 hrs (13 cells, 4 cords
799 cells); 2-4 hrs (9 cells, 3 cords) and 4-6 hrs (10 cells, 4 cords). Representative traces of
800 motoneuron firing in a control motoneuron or after 4 hours in the continuous presence of
801 gabazine in the bath. Lower trace shows the ramp protocol applied to evoke
802 motoneuron firing (**A**). Box and dot plots showing quartile distribution and individual
803 values for of the rheobase (**B1**), threshold (**B2**), resting membrane potential (**B3**), and
804 input resistance (**B4**) in control; 0-2, 2-4 and 4-6 hrs in gabazine. Inset of B3 shows
805 results for cords that were never treated with gabazine but cells were recorded in the
806 first, second or third 2hr period. (**C and D**) Interneuron excitability was measured in
807 isolated spinal cords using the same protocol as above to assess rheobase and
808 threshold in the absence (control – 22 cells, 8 cords) or in the continuous presence of
809 gabazine (10 mM) at 3 different blockade periods: 0-2 hrs (14 cells, 5 cords), 2-4 hrs (9
810 cells, 3 cords) and 4-6 hrs (6 cells, 3 cords). Representative traces of firing in a control
811 interneuron or after 4 hours in the continuous presence of gabazine in the bath. Lower
812 trace shows the ramp protocol applied to evoke interneuron firing (**C**). Box and dot plots
813 showing the value of the rheobase (**D1**), threshold (**D2**), resting membrane potential

(**D3**), or input resistance (**D4**) in control; 0-2, 2-4 and 4-6 hrs periods in the presence of gabazine. Inset of D3 shows results for cords that were never treated with gabazine but interneurons were recorded in the first, second or third 2hr period. Kruskal-Wallis method followed by a post-hoc Dunn test was used to asses statistical significance.*P<0.05; ** P<0.01 and ***P<0.001. For all plots, the continuous line represents the median and the dotted line represent the mean of the sample.

Figure 5. Changes in voltage-gated channel expression following *in ovo* gabazine treatment. Western blots showing changes in the expression of voltage-dependent Na^+ channels (Nav1.2) and inactivating K^+ channels (Kv4.2) in the chick embryo spinal cord following 12 hrs **(A)** or 6 hrs **(B)** of $GABA_A$ receptor blockade *in ovo*.

Figure 6. Chronic reductions in quantal GABA release that mediate synaptic upscaling do not trigger changes in motoneuron excitability. Whole cell voltage and current clamp recordings from motoneurons were obtained from isolated spinal cords before (14 cells, 6 cords) or after 2hrs of the nicotinic receptor antagonist (16cells, 6 cords) DHβE (10 mM). Representative traces are shown. Top black trace - mPSC before DHβE addition; bottom gray trace - following nicotinic receptor inhibition with DHβE addition (**A**). Despite this, no changes in intrinsic cell excitability were measured after 2 hours of DHβE treatment. Whole cell current clamp recording during a ramp test showing representative traces of motoneurons, before and after 2hrs of DHβE (**B**). The ramp protocol was applied to evaluate rheobase current and voltage threshold. Box and

dot plots show that rheobase (**C**) threshold (**D**), RMP (**E**), and input resistance (**F**) were not different after two hours of DHβE compared to controls. A Mann-Whitney test was used to quantified statistical significance. For all plots, the continuous line represents the median and the dotted line represent the mean of the sample.

Figure 7. Synaptic scaling does not contribute to the homeostatic recovery of SNA-generated movements. (A) Representative traces of the average mPSCs from single interneurons in control conditions or after 6 hours of *in vivo* gabazine treatment (left side). Box and dot plots (right side) showing quartile distribution and individual values for of AMPAergic and GABAergic miniature postsynaptic current amplitudes (mPSCs) from embryonic spinal interneurons in control conditions (12 cells, 4 cords) and after 6 hrs of chronic treatment with 10 μM gabazine (15 cells, 5 cords). **(B)** Box and dot plots showing AMPAergic and GABAergic mPSC frequency from embryonic spinal interneurons neurons in control conditions and after 6 hrs of chronic treatment with gabazine. **(C)** Representative traces of the average mPSCs from single motoneurons in control conditions or after 6 hours of gabazine treatment (left side). Box and dot plots (right side) showing quartile distribution and individual values for of AMPAergic and GABAergic miniature postsynaptic current amplitudes (mPSCs) from embryonic spinal motoneurons in control conditions (15 cells, 5 cords) and after 6 hrs of chronic treatment with 10 μM gabazine (14 cells, 5 cords). **(B)** Box and dot plots showing AMPAergic and GABAergic mPSC frequency from embryonic spinal motoneurons in control conditions and after 6 hrs of chronic treatment with gabazine.

For all plots, the continuous line represents the median and the dotted line represent the mean of the sample. Sample size is indicated as (interneurons/chick embryos) in all plots.

Figure 8. Episodes of spontaneous network activity are delayed and then recover following Glutamatergic blockade. The interval between episodes of SNA are plotted against elapsed time for 3 different cords before and following treatment with CNQX and APV (20 and 50μM, respectively). Episode intervals are increased just after adding glutamate receptor antagonists, but then recover to a higher rate. Inset shows example traces of SNA from a cord before (black) and after bath addition of CNQX/APV (grey). Traces were filtered from 0.1Hz – 10KHz.

Figure 9. Motoneuron excitability increased following *in vitro* glutamatergic blockade. Motoneuron excitability was measured in isolated spinal cords using a ramp protocol from 0 to 200 pA in 1.2 sec to assess rheobase current and voltage threshold in the absence (control – 33 cells, 12 cords) or in the continuous presence of CNQX 10 mM and APV 50 mM at 3 different blockade periods: 0-2 hrs (11 cells, 4 cords); 2-4 hours (8 cells, 3 cords) and 4-6 hrs (12 cells, 4 cords). Representative traces of motoneuron firing in control and after 3 hours of continuous CNQX and APV in the bath (**A**). Box and dot plots showing quartile distribution and individual values for of the rheobase (**B**), threshold (**C**), resting membrane potential (**D**), and input resistance (**E**) in isolated spinal cord motoneurons. For all plots, the continuous line represents the

median and the dotted line represent the mean of the sample. * P<0.05, ** P<0.01, *** P<0.001, ANOVA with Bonferroni Post Hoc test.

Figure 10. Interneuron excitability increased following *in vitro* glutamatergic blockade. Interneuron excitability was measured in isolated spinal cords with the same protocol used for motoneurons to calculate rheobase current and voltage threshold in controls without drugs (22 cells, 8 cords, these are the same values as in Figure 4 control interneurons) or in the continuous presence of CNQX 10 mM and APV 50 mM at 3 different blockade periods: 0-2 hours (8 cells, 3 cords), 2-4 hours (7 cells, 3 cords) and 4-6 hours (6 cells, 3 cords). (**A**) Representative traces of interneuron firing in control with no drugs and after 5 hours of continuous CNQX and APV in the bath. Box and dot plots showing quartile distribution and individual values of rheobase (**B**), threshold (**C**), resting membrane potential (**D**), and input resistance (**E**) in isolated spinal cord. For all plots, the continuous line represents the median and the dotted line represent the mean of the sample. Sample size is indicated as (interneurons/chick embryos) in all plots. *** P<0.001, ANOVA with Bonferroni Post Hoc test.

Table 1. Cellular excitability measures for motoneurons and interneurons following different treatments *in vitro* and in vivo. Numbers in bold are show significant difference with controls. Measures are averages +/- standard errors.

905
906
907
908
909
910
911
912

913 **Extended Data**

914

915 **Figure 3 - 1**

916 SNA episode duration is reduced following neurotransmitter receptor blockade.
917 Following the bath addition of gabazine episode duration is reduced compared to that
918 before adding the drug. Individual dots represent duration of a single episode before
919 and after drug addition to an individual cord.

920

921 **Figure 7 - 1**

922 Decay time constants (τ) for GABA mPSCs, A) before (τ =17.06 ± 0.83 ms; n=15) and
923 B) after (τ = 15.7 ± 0.86 ms; n=14) the addition of gabazine to the bath - were not
924 significantly different (p=0.26). C) τ for AMPA mPSCs before (τ = 3.16 ± 0.19 ms;
925 n=15) and D) after addition of gabazine to the bath (τ =3.39 ± 0.17 n=14) are shown. No
926 significant difference was observed (p=0.39).

927

928

929 **Figure 8 - 1**

930 SNA episode duration is reduced following neurotransmitter receptor blockade.
931 Following the bath addition of CNQX/APV episode duration is reduced compared to that
932 before adding the drugs. Individual dots represent duration of a single episode before
933 and after drug addition to an individual cord.

934

Figure 1

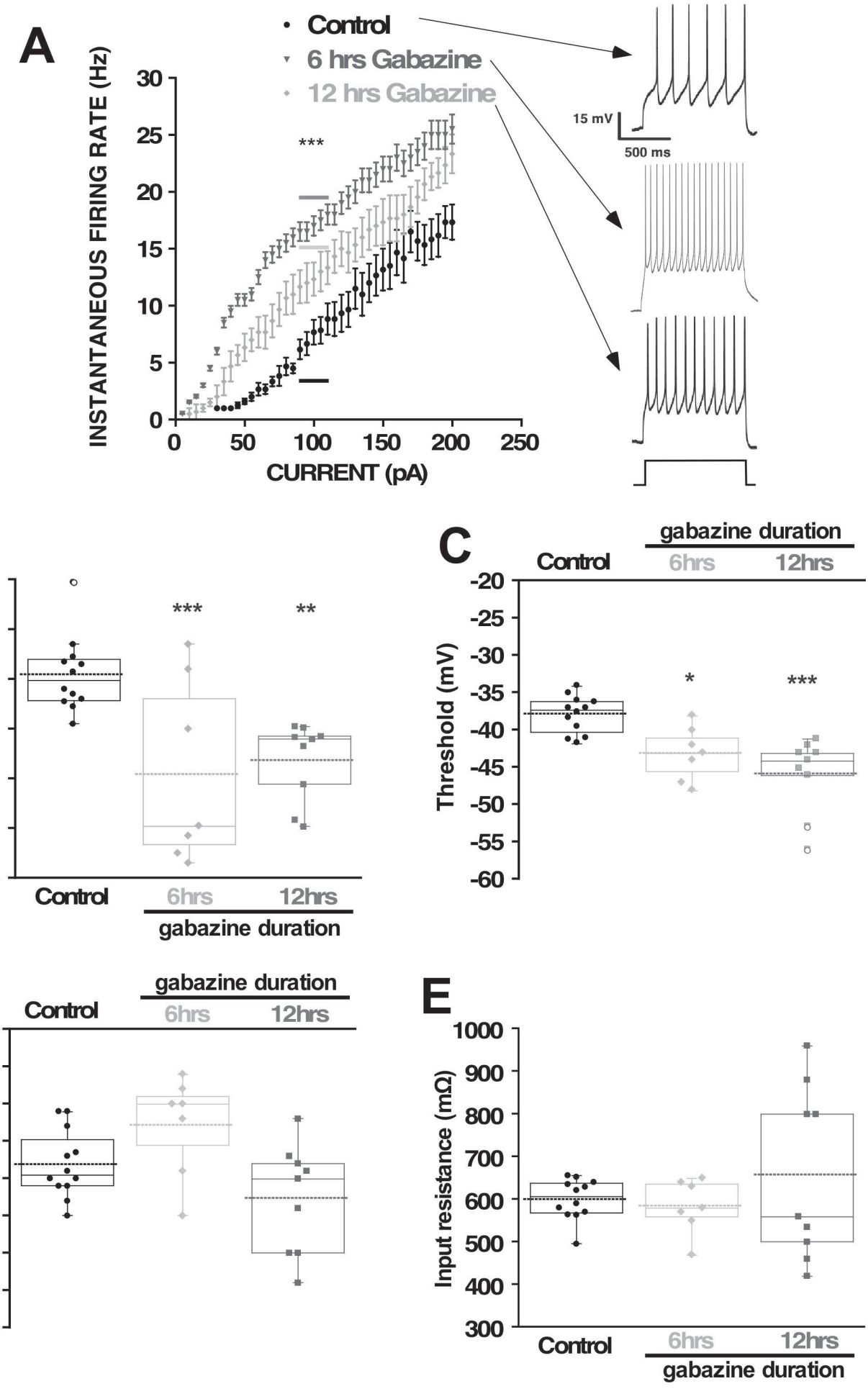

Figure 2

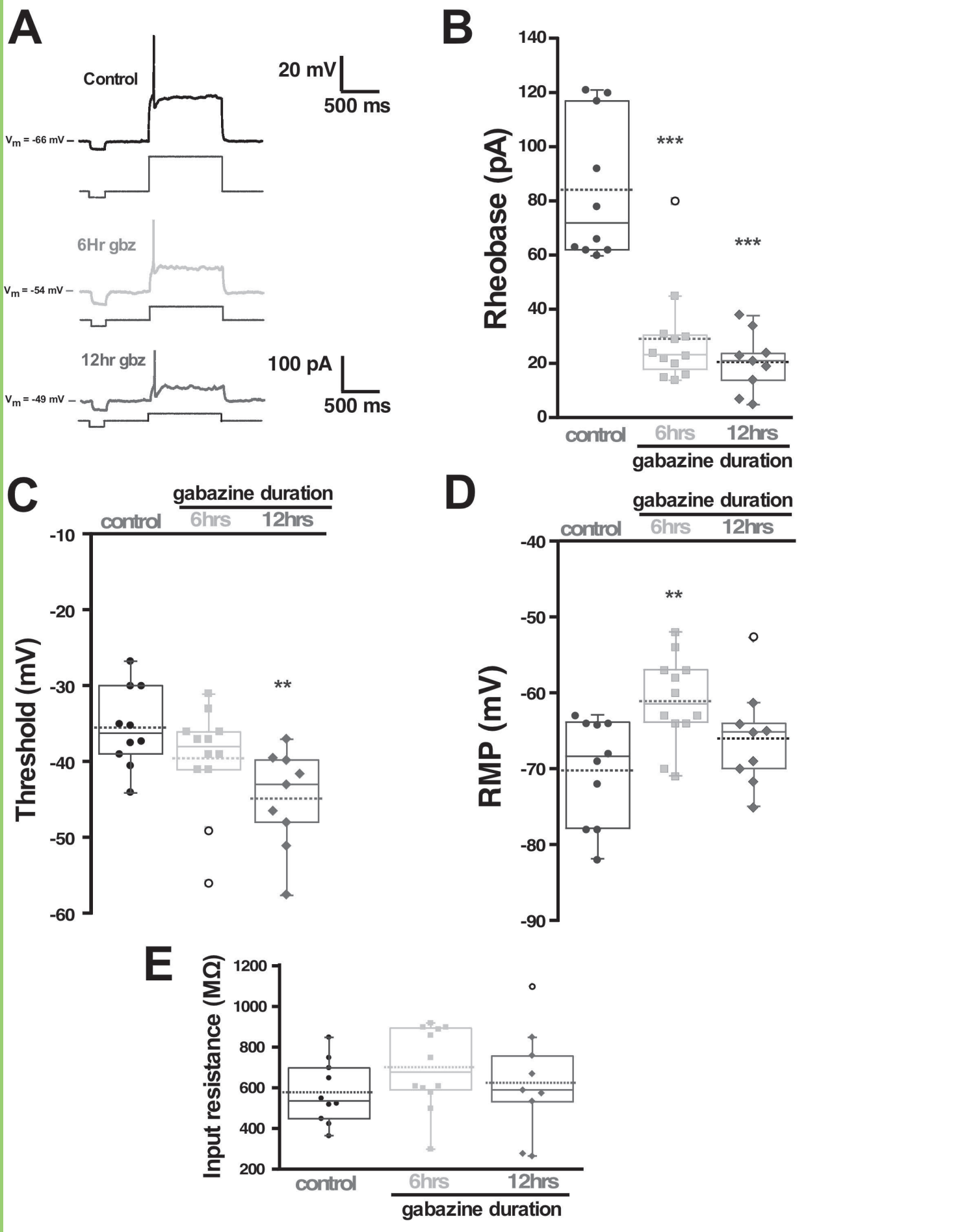

Figure 3

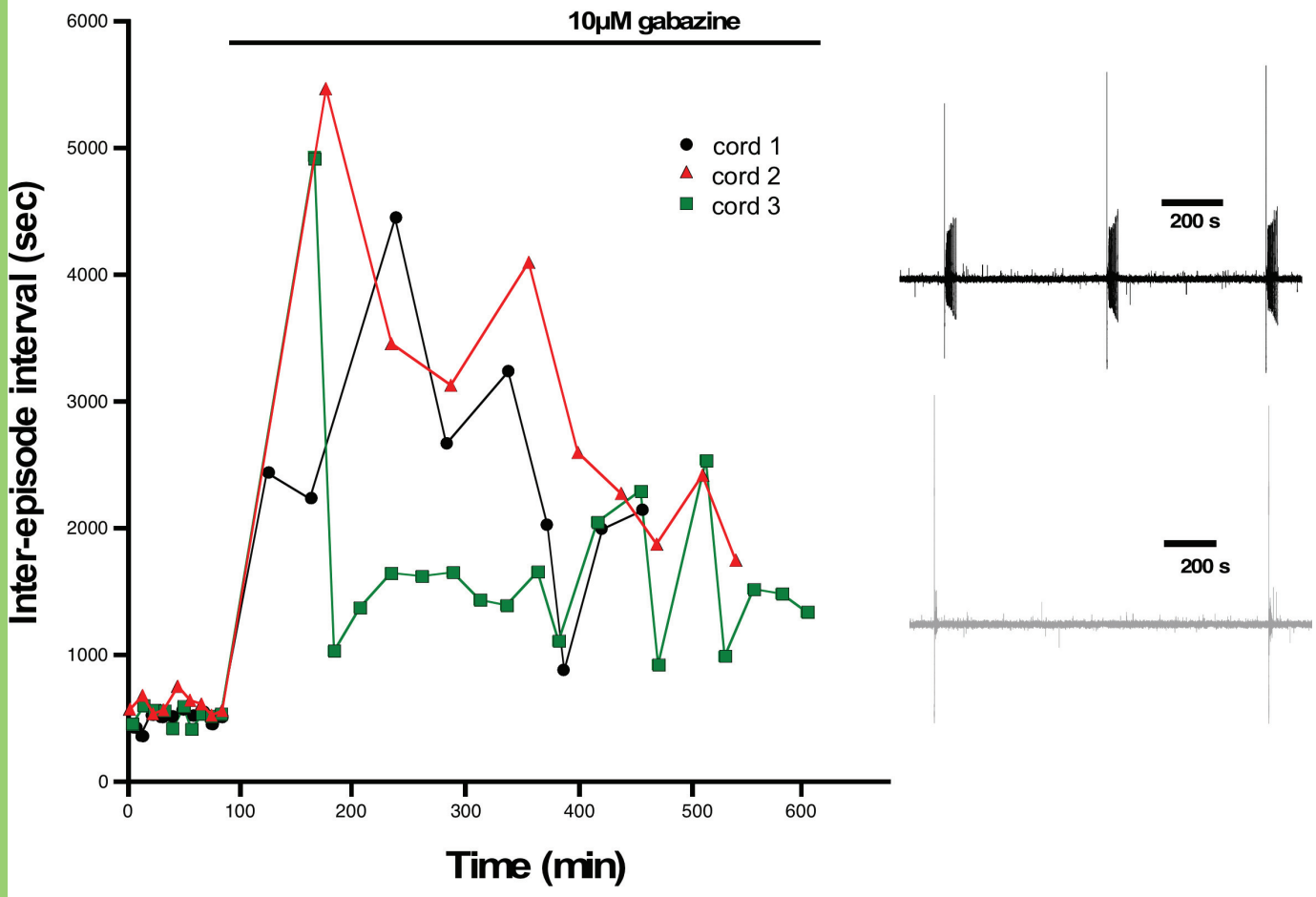

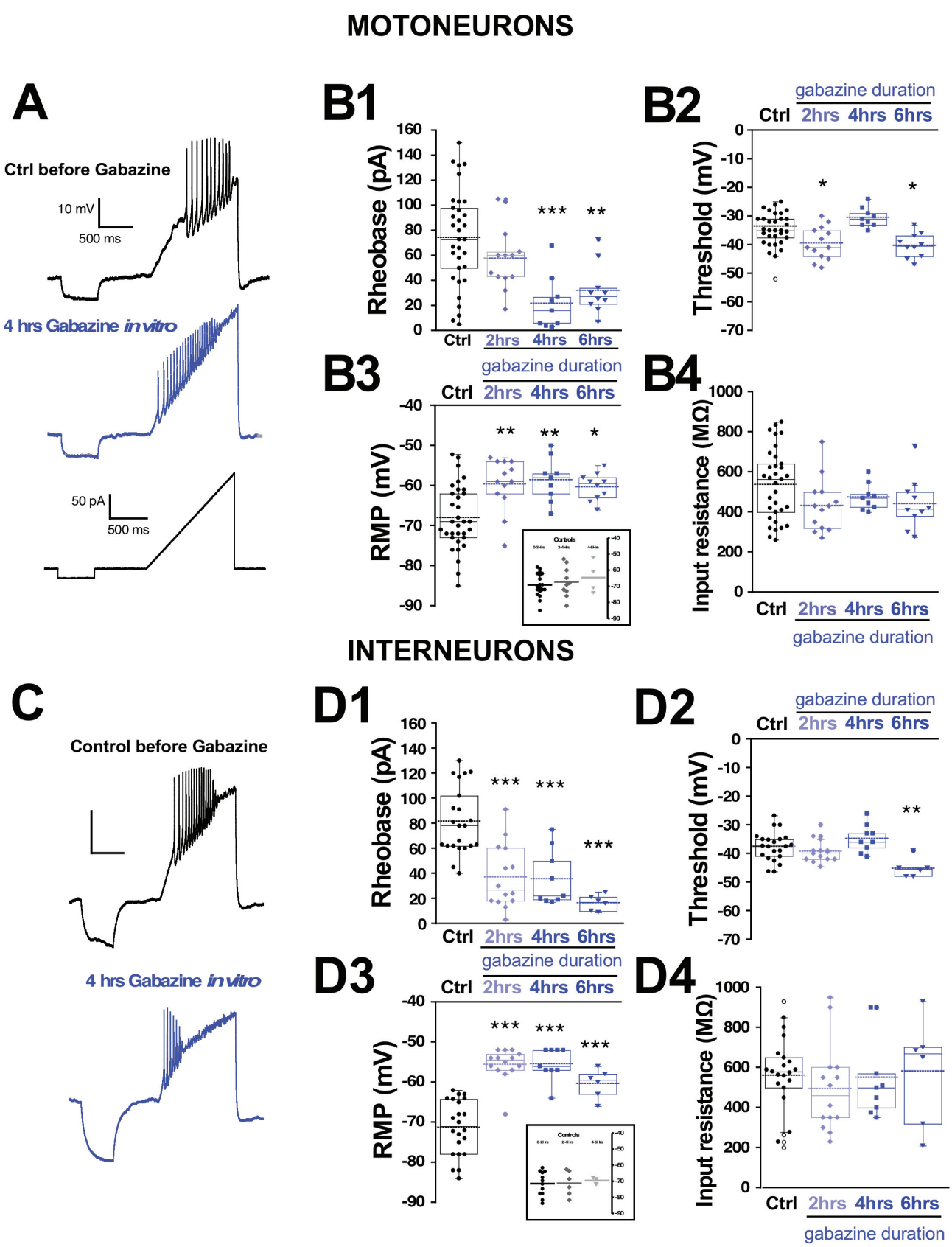

Figure 4

Figure 5

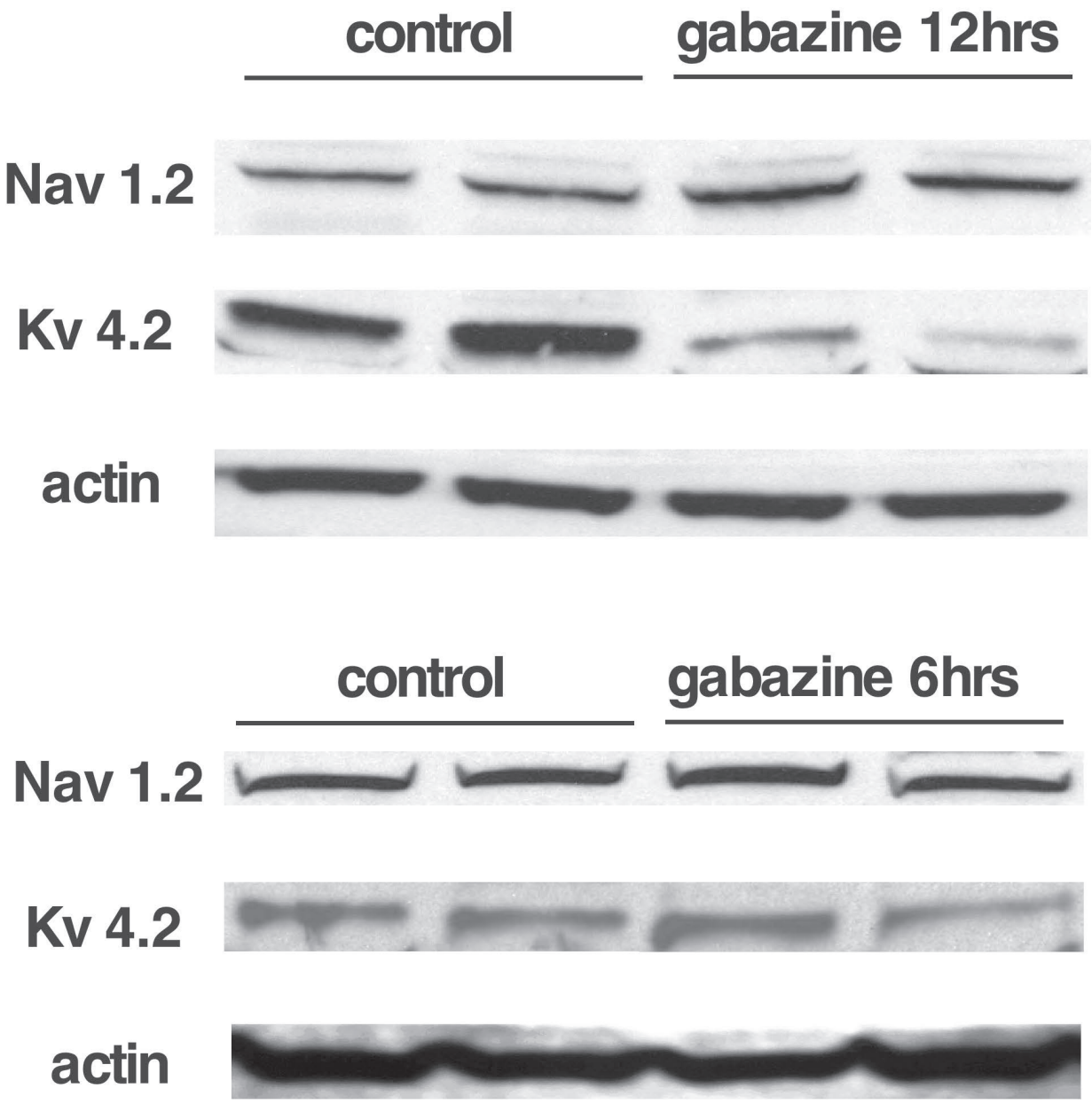

Figure 6

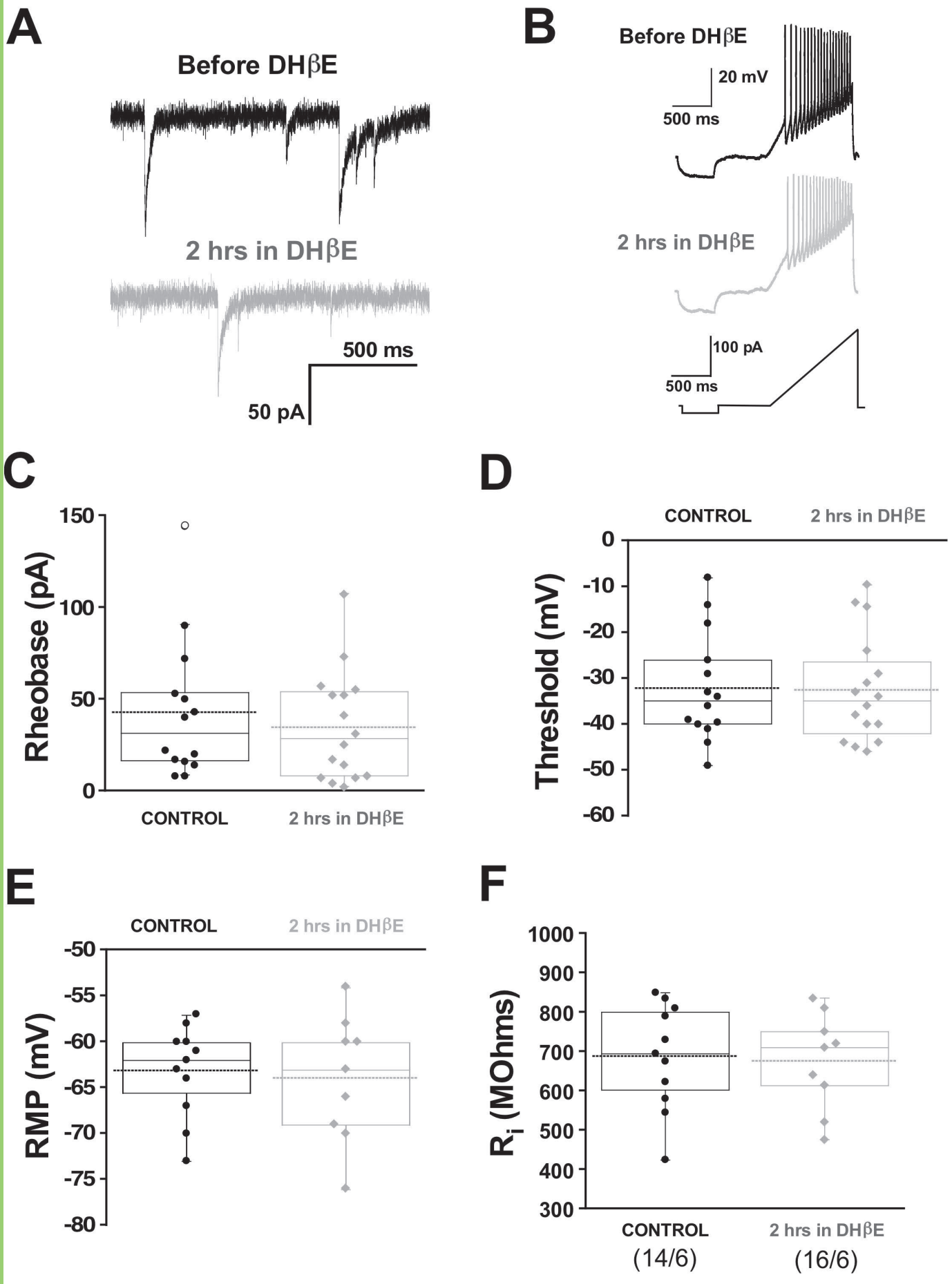

Figure 7

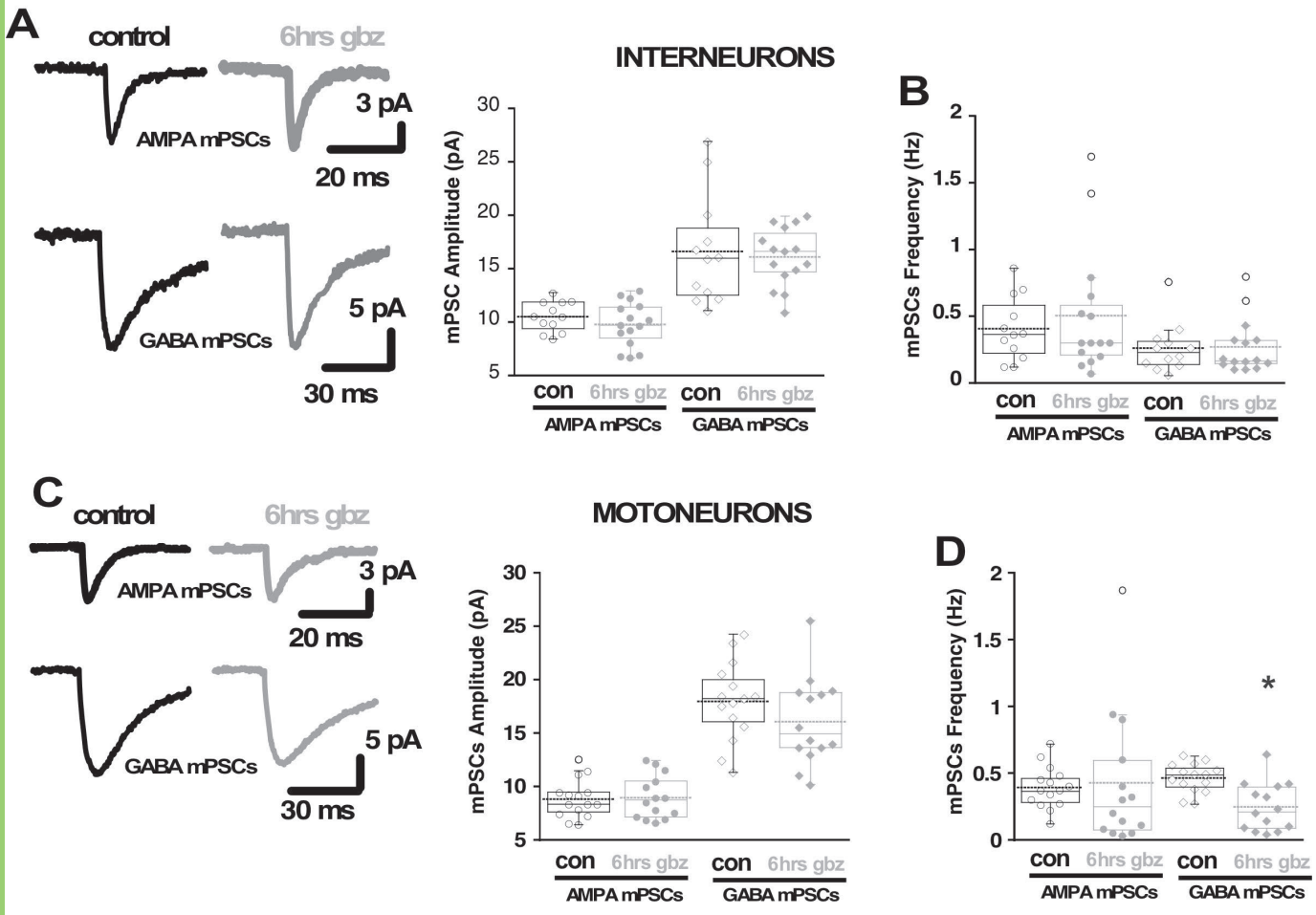

Figure 8

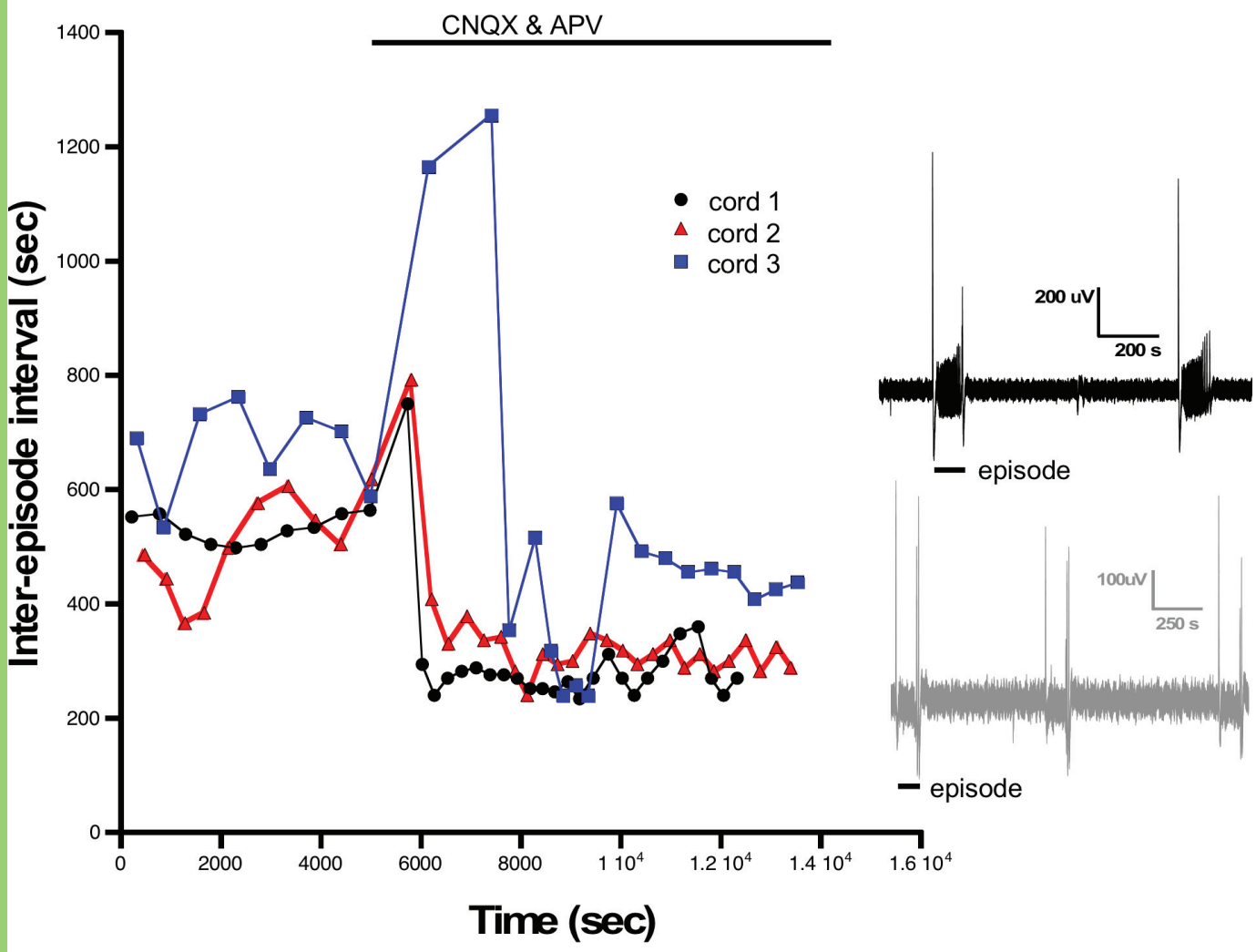

Figure 9

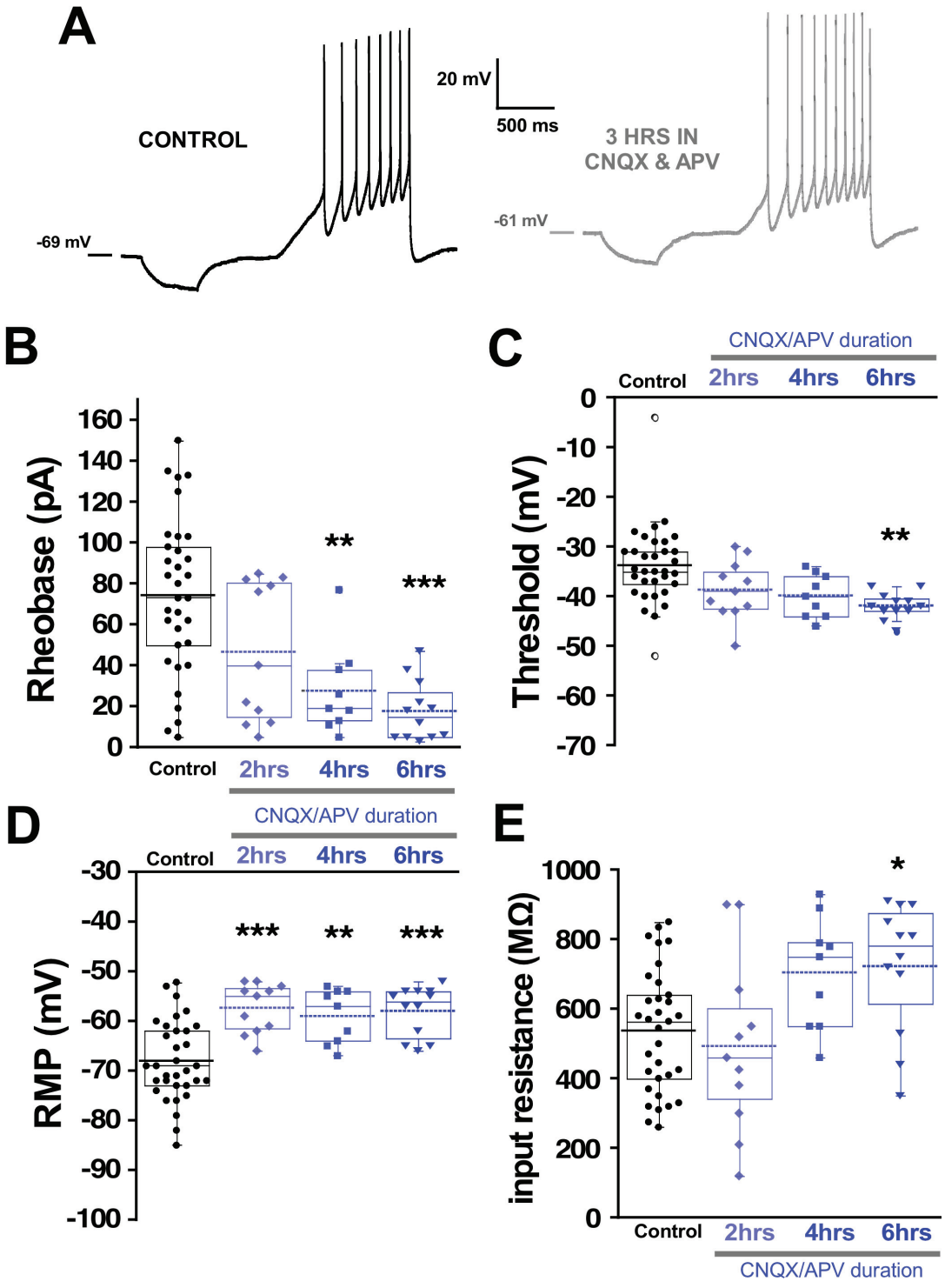

Figure 10

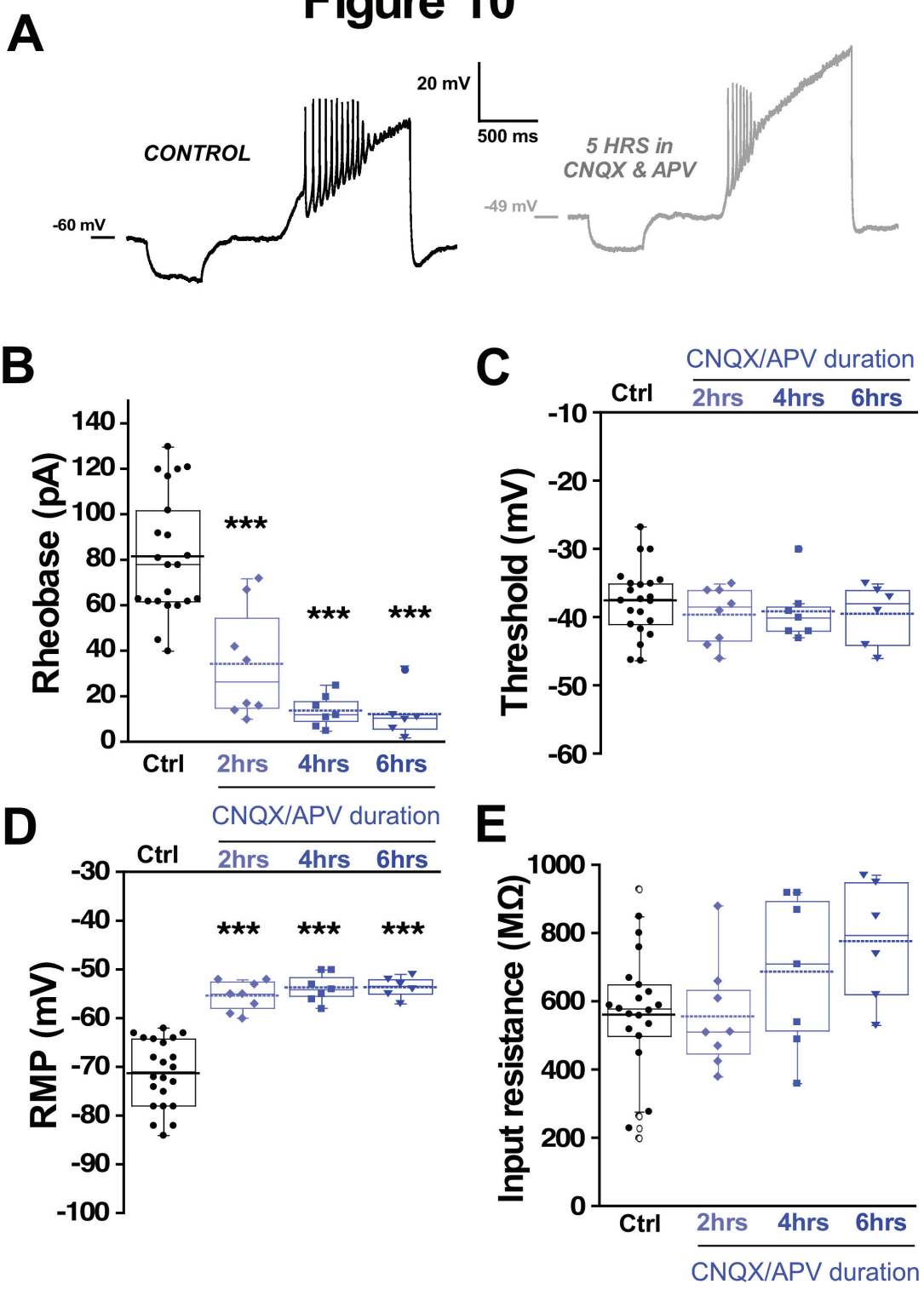

Condition	Motoneuron Rheobase (pA)	Motoneuron V_m-V_t (mV)	Motoneuron RMP (mV)	Motoneuron Rm (MΩ)	Interneuron Rheobase (pA)	Interneuron V_m-V_t (mV)	Interneuron RMP (mV)	Interneuron Rm (MΩ)
Controls *in vivo*	81.8 ± 4.3	30.3 ± 1.6	-68.1 ± 1.3	599.6 ± 13.8	84.1 ± 8.3	34.7 ± 2.7	-70.2 ± 2.2	578.5 ± 49.0
$GABA_AR$ Blockers 6 hrs *in vivo*	**41.7 ± 14.0**	**19.7 ± 3.1**	-62.9 ± 2.5	584.3 ± 23.9	**29.1 ± 5.3**	21.5 ± 2.1	**-61.1 ± 1.7**	701.7 ± 57.3
$GABA_AR$ Blockers 12 hrs *in vivo*	**47.3±5.3**	26.8 ± 2.9	-72.7 ± 2.4	657.2 ± 67.3	**20.6 ± 3.7**	21.1 ± 2.3	-66.0 ± 2.2	624.8 ± 88.1
Controls *in vitro*	74.3 ± 6.7	34.5 ± 2.1	-68.0 ± 1.4	537.2 ± 30.6	81.6 ± 5.7	33.7 ± 1.8	-71.3 ± 1.5	560.8 ± 40.9
$GABA_AR$ Blockers 0-2 hrs *in vitro*	57.8 ± 7.1	20.3 ± 1.3	**-59.6 ± 1.8**	432.3 ± 37.3	**37.0 ± 6.9**	**16.3 ± 1.4**	**-55.6 ± 1.1**	494.6 ± 58.7
$GABA_AR$ Blockers 2-4 hrs *in vitro*	**21.8 ± 7.2**	**28.1 ± 1.8**	**-58.6 ± 1.8**	474.4 ± 22.0	**35.7 ± 7.4**	**21.6 ± 1.4**	**-55.4 ± 1.3**	550.56 ± 70.0
$GABA_AR$ Blockers 4-6 hrs *in vitro*	**32.1 ± 6.3**	**20.0 ± 1.4**	**-60.3 ± 1.1**	442.0 ± 41.0	**16.5 ± 2.5**	**15.8 ± 1.5**	**-60.3 ± 1.5**	582.5 ± 109.13
GluR Blockers 0-2 hrs *in vitro*	46.6 ± 10.3	**18.6 ± 7.2**	**-57.4 ± 1.5**	492.7 ± 76.1	**34.3 ± 8.7**	**15.8 ± 1.1**	**-55.4 ± 1.1**	555.9 ± 56.4
GluR Blockers 2-4 hrs in vitro	**27.6 ± 7.4**	**19.1 ± 1.8**	**-59.0 ± 1.8**	704.4 ± 54.3	**13.7 ± 2.7**	**14.6 ± 1.5**	**-53.7 ± 1.1**	687.1 ± 85.9
GluR Blockers 4-6 hrs in vitro	**17.7 ± 4.2**	**16.1 ± 1.9**	**-58.0 ± 1.5**	**722.5 ± 54.1**	**12.2 ± 4.2**	**14.2 ± 1.1**	**-53.7 ± 0.9**	776.7 ± 72.9